

## Control of Mesoporous Silica Nanostructures and Pore-Architectures Using a Thickener and a Gelator

Yonggang Yang, Masahiro Suzuki, Sanae Owa, Hirofusa Shirai,  
and Kenji Hanabusa\*

Contribution from the Department of Functional Polymer Science, Faculty of Textile Science  
and Technology, Shinshu University, Ueda 386-8567, Japan

Received June 15, 2006; Revised Manuscript Received November 17, 2006; E-mail: hanaken@gipct.shinshu-u.ac.jp

**Abstract:** A chiral cationic thickener L-ValPyBr, which was able to enhance the viscosity of water and form loosely physical gel in mixtures of water and alcohols, was synthesized. Sol-gel polymerization of TEOS was carried out in mixtures of water and alcohols under basic conditions using the self-assemblies of L-ValPyBr as template. The left-handed twisted mesoporous silica nanoribbons, which were constructed by nanotubes in monolayer, were obtained, and they tended to self-assemble into bundle structure. Stirring under the preparation process played an important role in the formation of this bundle structure. The obtained silica nanoribbons were uniform in width, thickness, and helical pitch without combining amorphous particles. The helical pitch and pore size of the mesoporous silica nanoribbons sensitively depended on the volume ratio of alcohols to water in the reaction mixtures. With increasing volume ratio of alcohols to water in the reaction mixture, the morphologies of the obtained silica changed from left-handed twisted ribbon to coiled ribbon, then to tubular structure. A compound L-ValPyPF<sub>6</sub>, structurally related to thickener L-ValPyBr, was able to form physical gel in ethanol, THF, acetonitrile, and the mixtures of ethanol and water. Left-handed multiple helical mesoporous silica nanofibers were prepared by using the self-assemblies of L-ValPyPF<sub>6</sub> as template in mixtures of water and alcohols under basic conditions. By controlling both the volume ratio of ethanol to water and the weight ratio of L-ValPyPF<sub>6</sub> to TEOS, two- or three-dimensional pore-architecture constructed by porous chiral nanotubes was obtained.

### Introduction

Recently, the control of the morphological shapes and internal pore-architectures of mesoporous silica has become a hot topic. Mesoporous silica balls,<sup>1</sup> fibers,<sup>2</sup> and ribbons<sup>3–5</sup> have been prepared by many research groups. These structures have potential applications for chemical separations, catalysis, and photonic devices.<sup>6</sup> Among the morphologies, the one-dimensional (1D) morphologies are particularly important for applications. They can serve as waveguides<sup>7</sup> and as laser materials after doping with dyes.<sup>8</sup> Although the mesoporous fibers and ribbons have been prepared using the self-assemblies of surfactants<sup>3,9</sup> or amphiphilic block copolymers<sup>10</sup> as templates, it is still hard to control them to be uniform in nanosize.

Besides the morphologies, the control of the internal pore-architecture of mesoporous particles is also essentially needed for the applications of these materials. Recently, both hierarchical<sup>11–13</sup>

and chiral<sup>14–16</sup> mesoporous materials have attracted the interest of many researchers. Chiral mesoporous silica has been successfully prepared by using a chiral anionic surfactant,<sup>15</sup> sodium *N*-acyl-L-alanate with an aminosilane or a quaternized aminosilane as a co-structure-directing agent. However, both left- and right-handed helical structures were identified in the products. Recently, we succeeded in preparing inner helical mesoporous silica nanofibers<sup>16</sup> and twisted mesoporous silica ribbons<sup>17</sup> using the self-assemblies of cationic gelators as templates. Moreover, various single-handed helical mesoporous nanostructures have been prepared using the self-assemblies of a chiral cationic surfactant as templates: for instance, double helical mesoporous nanofiber, single-stranded loosely coiled mesoporous nanofiber,

- (1) Lu, Y.; Fan, H.; Stump, A.; Ward, T. L.; Rieker, T.; Brinker, J. *Nature* **1999**, *398*, 223.
- (2) (a) Yang, H.; Coombs, N.; Ozin, G. A. *Nature* **1997**, *386*, 692. (b) Schacht, S.; Huo, Q.; Voigt-Martin, I. G.; Stucky, G. D.; Schüth, F. *Science* **1996**, *273*, 768. (c) Mann, S.; Ozin, G. A. *Nature* **1996**, *382*, 313. (d) Kleitz, F.; Marlow, F.; Stucky, G. D.; Schüth, F. *Chem. Mater.* **2001**, *13*, 3587.
- (3) Wang, J.; Tsung, C.-K.; Hayward, R. C.; Wu, Y.; Stucky, G. D. *Angew. Chem., Int. Ed.* **2005**, *44*, 332.
- (4) Seddon, A. M.; Patel, H. M.; Burkett, S. L.; Mann, S. *Angew. Chem., Int. Ed.* **2002**, *41*, 2988.
- (5) Jung, J. H.; Shinkai, S.; Shimizu, T. *Chem. Rec.* **2003**, *3*, 212.
- (6) Davis, M. E. *Nature* **2002**, *417*, 813.
- (7) Huo, Q.; Zhao, D.; Feng, J.; Weston, K.; Buratto, S. K.; Stucky, G. D.; Schacht, S.; Schüth, F. *Adv. Mater.* **1997**, *9*, 974.

- (8) Marlow, F.; McGehee, M.; Zhao, D.; Chmelka, B.; Stucky, G. D. *Adv. Mater.* **1999**, *11*, 632.
- (9) (a) Lin, H.-P.; Liu, S.-B.; Mou, C.-Y.; Tang, C.-Y. *Chem. Commun.* **1999**, 583. (b) Marlow, F.; Spliethoff, B.; Tesche, B.; Zhao, D. *Adv. Mater.* **2000**, *12*, 961.
- (10) Goto, Y.; Inagaki, S. *Chem. Commun.* **2002**, 2410.
- (11) Kuang, D.; Brezesinski, T.; Smarsly, B. *J. Am. Chem. Soc.* **2004**, *126*, 10534.
- (12) Nakanishi, K.; Kobayashi, Y.; Amatani, T.; Hirao, K.; Kodaira, T. *Chem. Mater.* **2004**, *16*, 3652.
- (13) Antonietti, M.; Ozin, G. A. *Chem.-Eur. J.* **2004**, *10*, 28.
- (14) Gier, T. E.; Bu, X.; Feng, P.; Stucky, G. D. *Nature* **1998**, *395*, 154.
- (15) Che, S.; Liu, Z.; Ohsuna, T.; Sakamoto, K.; Terasaki, O.; Tatsumi, T. *Nature* **2004**, *429*, 281.
- (16) Yang, Y.; Suzuki, M.; Kimura, M.; Shirai, H.; Kurose, A.; Hanabusa, K. *Chem. Commun.* **2005**, 2032.
- (17) Yang, Y.; Suzuki, M.; Owa, S.; Shirai, H.; Hanabusa, K. *Chem. Commun.* **2005**, 4462.

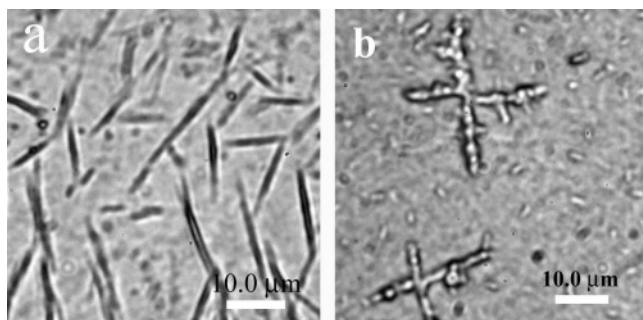


**Figure 1.** Optical micrograph images of the L-ValPyBr xerogels. (a) Xerogel obtained from viscous aqueous solution (30 mg of L-ValPyBr in 1.0 mL of H<sub>2</sub>O); (b) xerogel obtained from loose gel in the mixture of water and ethanol (30 mg of L-ValPyBr in 1.0 mL of H<sub>2</sub>O and 0.2 mL of ethanol).

and twisted ribbon.<sup>17</sup> They should be suitable for separation of enantiomers or as chiral catalysts. Here, we focused on self-assembly of thickener<sup>18,19</sup> as a new kind of template to control both the morphological shapes and the pore-architectures of mesoporous silica. Meanwhile, a gelator, structurally related to this thickener, was also prepared. Also, sol-gel transcriptions were carried out using the self-assemblies of the gelator. Because two-dimensional (2D) and three-dimensional (3D) chiral pore-architectures, which are supposed to show high surface area and accessibility, are more suitable for applications, we tried to prepare 2D and 3D chiral mesopores by controlling the reaction conditions.

## Results and Discussion

**Physical Properties of L-ValPyBr.** The syntheses of L-ValPyBr and L-ValPyPF<sub>6</sub> are shown in the Supporting Information (Scheme S1). L-ValPyBr shows interesting self-assembly properties to form a viscous solution in water and give loose physical gel in mixtures of water and alcohols such as methanol, ethanol, 1-propanol, and 2-propanol. The viscosity of the solution prepared from 20 mg of L-ValPyBr and 1.0 mL of pure water is 180 cP at 2.0 RPM at room temperature.

Figure 1 shows the optical micrograph images of the L-ValPyBr xerogels obtained both in water and in the mixture of ethanol and water. When 30 mg of L-ValPyBr was dissolved in 1.0 mL of water, a viscous solution was obtained. Optical micrography observation implied that many needle-like short rods were floating in the solution (Figure 1a). When 0.2 mL of ethanol was added into this viscous aqueous solution, a translucent loose gel was obtained. When the dried sample after removing solvent was observed, a three-dimensional network was recognized (Figure 1b). When the volume ratio of ethanol to water was higher than 1:1, transparent solutions were formed instead of translucent loose gels.

**Sol-Gel Polycondensation of Tetraethoxy Orthosilicate (TEOS) in Mixtures of 2-Propanol and Water.** First, we carried out sol-gel polymerization of TEOS in mixtures of 2-propanol and water using thickener L-ValPyBr. To visually study the morphological shapes and internal pore-architectures of silica, we used field emission scanning electron microscopy (FESEM) and transmission electron microscopy (TEM). Before FESEM images were taken, 10 nm Pt-Pd metal was covered on the surface of the silica nanostructures. Figure 2a and b shows

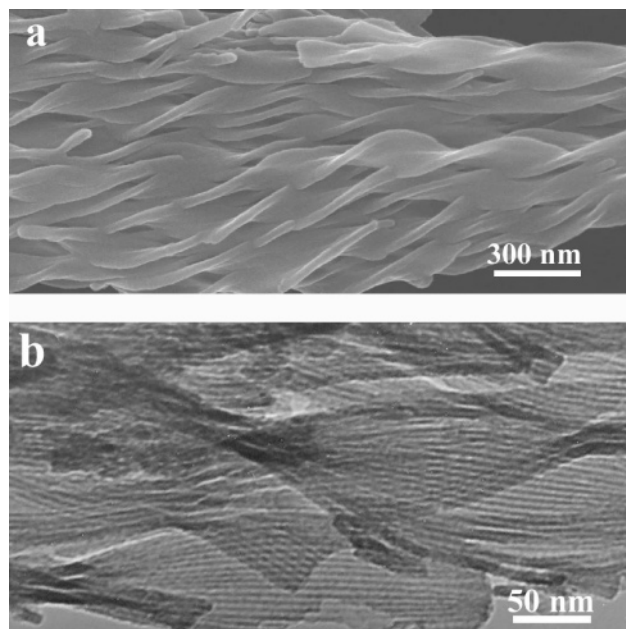


**Figure 2.** FESEM (a) and TEM (b) images of twisted mesoporous silica nanoribbons after calcination. Preparation condition: 10 mg of L-ValPyBr, 0.4 mL of 2-propanol, 0.6 mL of 10.0 wt % NH<sub>3</sub> aq, and 20 mg of TEOS.

the left-handed twisted silica nanoribbons, which were prepared from 10 mg of L-ValPyBr, 0.4 mL of 2-propanol, 0.6 mL of 10.0 wt % NH<sub>3</sub> aq, and 20 mg of TEOS after calcination. These nanoribbons have a uniform width of ca. 100 nm, a uniform thickness of ca. 7 nm, and even a uniform helical pitch of ca. 880 nm (Figure 2). The inner diameters of the channels are around 3 nm after calcination (Figure 2b). Additionally, the TEM image also indicated that the mesoporous nanoribbons were constructed by nanotubes in monolayer. The nanoribbons were so thermally stable that the mesopores remained after being calcined at 550 °C for 5 h. The channels were parallel to each other and oriented to the length of the ribbons. The twisted ribbons exhibited a nitrogen Brunauer-Emmett-Teller (BET) surface area of 646 m<sup>2</sup>/g. The Barrett-Joyner-Halenda (BJH) pore size distribution plot determined from the adsorption branch showed a peak at 3.1 nm (Supporting Information, Figure S1). In the mixtures of 2-propanol and water, with increasing volume ratio of 2-propanol to water, the morphological shapes of obtained silica changed from short nanorods (Supporting Information, Figure S2) to left-handed twisted nanoribbons (Figure 2). Generally, the twisted silica nanoribbons tended to construct bundles. Meanwhile, it is found that the helical pitch of the twisted nanoribbons increased with increasing volume ratio of 2-propanol to water. For example, when the volume ratio of 2-propanol to water in the reaction mixture was 3:7, the helical pitch of the obtained silica ribbons was around 420 nm (Supporting Information, Figure S3).

**Sol-Gel Polycondensation of TEOS in Water.** For a better understanding of the formation of these mesoporous ribbons, we carried out the sol-gel transcription reactions in pure water. Figure 3 shows silica nanoribbons prepared from a mixture of 10 mg of L-ValPyBr, 1.0 mL of 5.0 wt % NH<sub>3</sub> aq, and 20 mg of TEOS after calcination. The silica nanoribbons were constructed with short nanorods. Typically, these rods were several micrometers in length in comparison to the previous nanoribbons with lengths of 30–40 μm and tended to assemble into ribbons.

(18) Shikata, T.; Ogata, D.; Hanabusa, K. *J. Phys. Chem. B* **2004**, *108*, 508.

(19) Ogata, D.; Shikata, T.; Hanabusa, K. *J. Phys. Chem. B* **2004**, *108*, 15503.

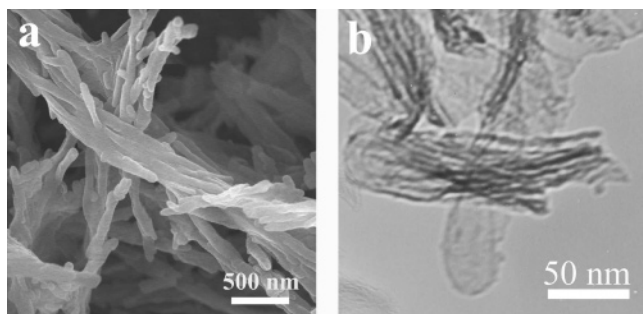


**Figure 3.** FESEM (a) and TEM (b) images of twisted silica ribbons constructed by short nanotubes after calcination. Preparation condition: 10 mg of L-ValPyBr, 1.0 mL of 5.0 wt %  $\text{NH}_3$  aq, and 20 mg of TEOS.

The TEM image indicates that many pore channels are twisted slightly and oriented to the axis of the nanorods (Figure 3b). The twisted ribbons exhibited a nitrogen BET surface area of  $394 \text{ m}^2/\text{g}$ , and the BJH pore size distribution plot shows an average pore size at 3.5 nm (Supporting Information, Figure S4).

Self-assemblies of surfactants,<sup>3</sup> lipids,<sup>4</sup> and gelators<sup>5,17</sup> have been used as the templates for mesoporous silica ribbons. When cationic surfactants were used, mesoporous ribbon with tracklike pore channels was obtained.<sup>3</sup> The channels were oriented perpendicularly to the length of the ribbon and hexagonally packed. When cationic lipids or gelators were used, two kinds of pore-architectures were obtained. One is lamellar mesostructure, in which mesopores were formed among silica ribbons.<sup>4,5</sup> The lamellar mesoporous silica ribbons were formed by the adsorption and polymerization of silica species on the surface of the self-assemblies of lipids or organogels. Although the ribbons were able to be controlled to be uniform in nanosize, unfortunately, this mesostructure does not show high thermostability. The other is the loosely coiled ribbon constructed by bundles of nanotubes.<sup>17</sup> The nanotubes are parallel to each other in monolayer. The ribbons were uniform in nanosize and did not combine with small particles. Unfortunately, they did not have uniform helical pitch. Considering the fact that the helical pitch of twisted nanoribbons was controllable by changing the ratio of 2-propanol and water in the reaction mixtures, the thickener L-ValPyBr should be the most interesting compound to control the pore-architectures of mesoporous silica nanoribbons.

**Sol–Gel Polycondensation of TEOS in Mixtures of Ethanol and Water.** To study the mechanism of the formation of mesoporous silica ribbons using the supramolecular self-assemblies of L-ValPyBr, the polymerization of TEOS was carried out in mixtures of water with other alcohols. The sol–gel polymerization of a mixture of 10 mg of L-ValPyBr, 0.4 mL of ethanol, 0.6 mL of 10.0 wt %  $\text{NH}_3$  aq, and 20 mg of TEOS gave the left-handed loosely helical mesoporous silica nanoribbons constructed by nanofibers and nanorods (Supporting Information, Figure S5). However, when the volume ratio of ethanol to water in the reaction mixture reached 1:1, the reaction mixture came into viscous solution again at room temperature, and flake-like silica particles were obtained after sol–gel polymerization (Supporting Information, Figure S6).

**Sol–Gel Polycondensation of TEOS in Mixtures of Methanol and Water.** The sol–gel transcription reaction was carried out in mixtures of methanol and water. Electron

micrographs of the obtained mesoporous silica are shown in the Supporting Information, Figure S7, where the top right values in the figures show the volume ratios of methanol to water. The morphologies of the obtained silicas depended on the volume ratio of methanol to water. The morphologies of the obtained silica nanostructures changed from loosely coiled ribbon (Figure S7a–c) to nanorod (Figure S7d) with increasing volume ratio of methanol to water. Silica nanoribbons (Figure S7a,b) were prepared from 10 mg of L-ValPyBr, 0.2 mL of methanol, 0.8 mL of 10.0 wt %  $\text{NH}_3$  aq, and 20 mg of TEOS. These ribbons were rebuilt into huge bundles structure (Figure S7a), which were constructed by nanotubes in monolayer (Figure S7b). They exhibited a nitrogen BET surface area of  $436 \text{ m}^2/\text{g}$ , and the BJH pore size distribution plot shows a peak at 4.4 nm (Supporting Information, Figure S8). The mesopores around 2–3 nm may be formed among the nanotubes within the nanoribbons. When the volume ratio of methanol to water was 3:7, helical bundles were identified, and the diameter of the bundles became thinner (Figure S7c). The twisted ribbons exhibited a nitrogen BET surface area of  $460 \text{ m}^2/\text{g}$ , and the pore size distribution plot showed a peak at 4.4 nm. If methanol more than the volume ratio of 3:7 was added into the reaction mixture, L-ValPyBr formed loose physical gel in the reaction mixture at 0 °C. However, only short nanorods were identified (Figure S7d).

**Proposed Mechanism.** Figure 4 illustrates the formation of mesoporous left-handed twisted mesoporous silica nanoribbons. First, single-strand helical self-assemblies are formed by the self-organization of thickener molecules in the solution. Second, silica oligomers are adsorbed onto the cationic surface of the supramolecular aggregates by the electronic interactions. Meanwhile, these aggregates self-assemble into left-handed helical ribbons. Finally, the silica oligomers are polymerized on the surface of single-strand helical supramolecular assemblies. The mesoporous silica nanoribbons are obtained after the obtained materials are extracted with methanol and calcined in air. Apparently, the organic self-assemblies go beyond inducing chirality and have a direct structure-inducing effect on the morphologies. This supposed mechanism is different from the previous one, in which silica oligomers are polymerized on the surface of lipid or gelator ribbons.<sup>4,5</sup>

**Sol–Gel Polycondensation of TEOS in Mixtures of 1-Propanol and Water.** To study the morphology and pore-architecture control of the self-assemblies of thickener L-ValPyBr in more detail, sol–gel transcription reactions were carried out in mixtures of 1-propanol and water. Figure 5 show electron micrographs of the obtained silicas, where the top right values in the figures show the volume ratios of 1-propanol to water. The volume ratio of 1-propanol to water was changed gradually in the reaction mixture. With increasing ratio of 1-propanol to water, the straight bundles (Figure 5a) changed to left-handed helical bundles (Figure 5c and d), then to left-handed helical tubular bundles (Figure 5e–h). These bundles are constructed by twisted ribbons, coiled ribbons, or tubes. The typical dimensions of the bundles were 20  $\mu\text{m}$  in length and 1.0  $\mu\text{m}$  in diameter. When the volume ratio of 1-propanol to water ranged from 2:8 to 4:6, only left-handed twisted ribbons were obtained (Figure 5a–d). However, the helical pitch of twisted ribbons increased with increasing volume ratio of 1-propanol to water. TEM image indicated that the nanoribbons were constructed

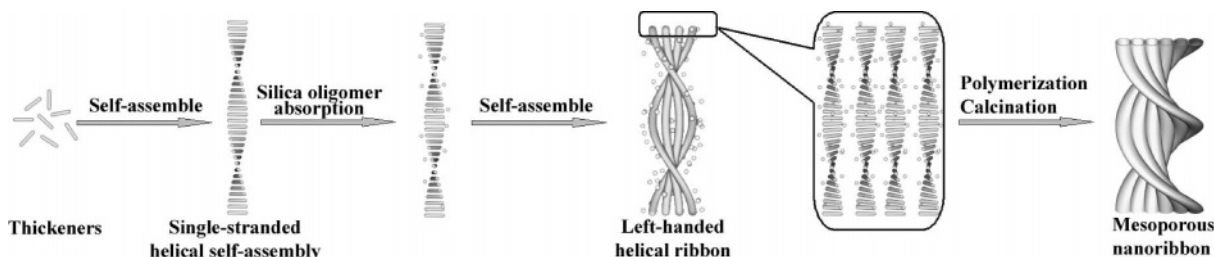


**Figure 4.** Schematic representation of formation of left-handed twisted mesoporous silica nanoribbons.

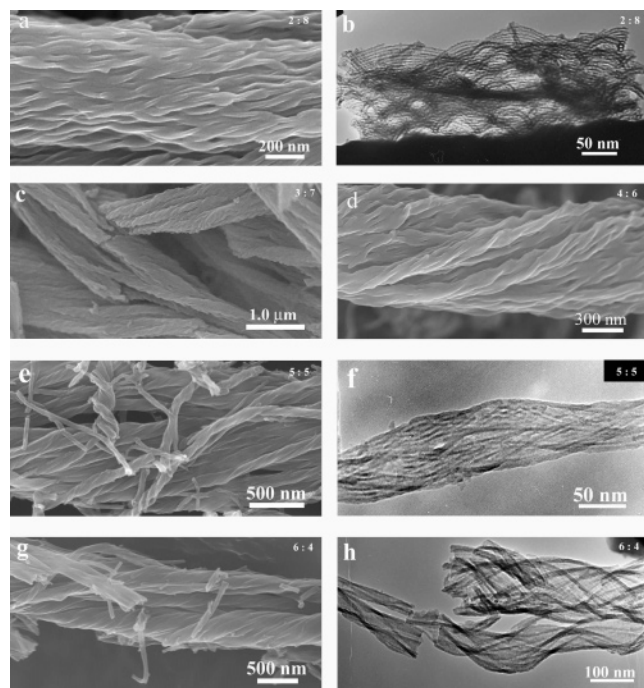


**Figure 5.** FESEM (a,c,d,e,g) and TEM (b,f,h) images of twisted and coiled silica ribbons after calcination. Preparation condition for (a) and (b): 10 mg of L-ValPyBr, 0.2 mL of 1-propanol, 0.8 mL of 10.0 wt %  $\text{NH}_3$  aq, and 20 mg of TEOS. Preparation condition for (c): 10 mg of L-ValPyBr, 0.3 mL of 1-propanol, 0.7 mL of 10.0 wt %  $\text{NH}_3$  aq, and 20 mg of TEOS. Preparation condition for (d): 10 mg of L-ValPyBr, 0.4 mL of 1-propanol, 0.6 mL of 10.0 wt %  $\text{NH}_3$  aq, and 20 mg of TEOS. Preparation condition for (e) and (f): 10 mg of L-ValPyBr, 0.5 mL of 1-propanol, 0.5 mL of 10.0 wt %  $\text{NH}_3$  aq, and 20 mg of TEOS. Preparation condition for (g) and (h): 10 mg of L-ValPyBr, 0.6 mL of 1-propanol, 0.4 mL of 10.0 wt %  $\text{NH}_3$  aq, and 20 mg of TEOS.

by nanotubes in monolayer and the inner pore diameter was around 4.0 nm (Figure 5b). The BET surface area of the silica shown in Figure 5a was 554  $\text{m}^2/\text{g}$  (Supporting Information, Figure S9). When the volume ratio of 1-propanol to water was 5:5 or higher, the twisted nanoribbons changed to tightly coiled nanoribbons (Figure 5e and f), and then to nanotubes (Figure 5g,h and Supporting Information, Figure S10). The BET surface area of the silica shown in Figure 7e was 315  $\text{m}^2/\text{g}$ , and the nitrogen BJH pore size distribution plot showed a peak at 5.0 nm (Supporting Information, Figure S11). When the volume ratio of 1-propanol to water was 6:4, the BET surface area of the obtained silica decreased to 199  $\text{m}^2/\text{g}$ , and the nitrogen BJH pore size increased to 5.5 nm. Many other mesopores ranging from 2 to 5 nm may be formed among the coiled ribbons (Figure 5h and Supporting Information, Figure S12). Both the BET results and the TEM images show that the pore size of these mesoporous silica nanoribbons increases with increasing volume ratio of 1-propanol to water. With increasing volume ratio of

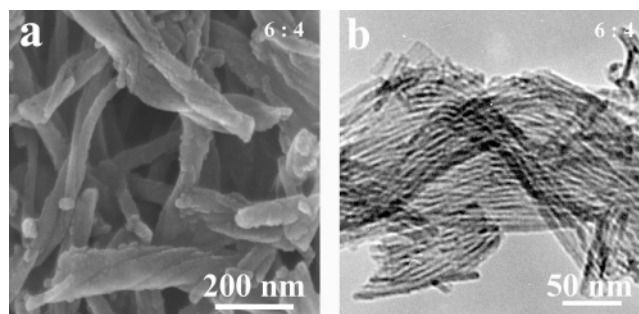


**Figure 6.** FESEM (a) and TEM (b) images of silica bundles after calcination. Preparation condition: 10 mg of L-ValPyBr, 0.6 mL of 1-propanol, 0.4 mL of 10.0 wt %  $\text{NH}_3$  aq, and 20 mg of TEOS.

1-propanol to water, the hydrolysis speed of TEOS and polycondensation speed of silica oligomers were retarded. Therefore, when the volume of 1-propanol to water is high enough, silica oligomers would adsorb on the surface of gel fiber bundles, not single-stranded supramolecular self-assemblies as shown in Figure 4. This should be the reason that the pore size of these mesoporous silica nanoribbons increases with increasing volume ratio of 1-propanol to water.

Recently, many groups have tried aligning one-dimensional nanostructures and building nanoparticles into more complicated structures for future applications.<sup>20</sup> We have also aligned nanofibers under stirring during the preparation process.<sup>21</sup> In this study, we found that stirring plays an important role in the formation of bundle structure. When sol-gel transcription reactions were carried out in 1-propanol/water (6:4) without stirring, the obtained helical bundles were only 50–100 nm in diameter and 0.3–2.0  $\mu\text{m}$  in length (Figure 6). As compared to the sample shown in Figure 5g, it seems that stirring can lengthen and align the self-assemblies of L-ValPyBr. The BET surface area of this sample was 291  $\text{m}^2/\text{g}$ , and the pore size was around 5.5 nm (Supporting Information, Figure S13). This result indicates that many other kinds of hierarchical structures may also be obtained simply by changing reaction conditions.

**Physical Properties of L-ValPyPF<sub>6</sub>.** Interesting helical mesoporous bundle structures were also prepared using gelator L-ValPyPF<sub>6</sub>, which was structurally related to thickener L-ValPyBr. L-ValPyPF<sub>6</sub> was able to gel water, ethanol, 1-propanol, 2-propanol, 1-butanol, ethyl acetate, THF, nitrobenzene, chloroform, acetonitrile, and the mixture of water and ethanol. In the FESEM picture of the xerogel prepared from the frozen sample of the ethanol gel (Supporting Information, Figure S14), nanofibers formed by twisted sheets were identified. The CD

(20) Xia, Y.; Yang, P.; Sun, Y.; Wu, Y.; Mayers, B.; Gates, B.; Yin, Y.; Kim, F.; Yan, H. *Adv. Mater.* **2003**, *15*, 353.

(21) Yang, Y.; Suzuki, M.; Fukui, H.; Shirai, H.; Hanabusa, K. *Chem. Mater.* **2006**, *18*, 1324.

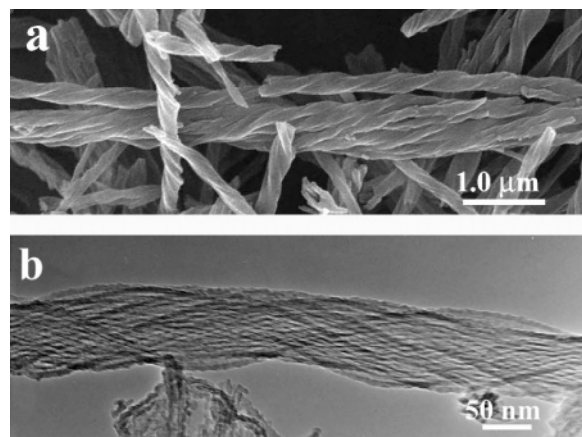


**Figure 7.** FESEM (a) and TEM (b) images of left-handed helical mesoporous silica bundles. Preparation condition: 10 mg of L-ValPyPF<sub>6</sub>, 0.6 mL of ethanol, 0.4 mL of 10.0 wt % NH<sub>3</sub> aq, and 20 mg of TEOS.

spectrum indicated that the molecules of L-ValPyPF<sub>6</sub> in the formed gel were cooperatively organized with helically stacked aromatic chromophores (Supporting Information, Figure S15).

Although we failed to obtain structured silica in pure water, silica nanostructures were successfully prepared in mixtures of alcohols and water. Figure 7 shows the FESEM and TEM images of the left-handed helical mesoporous silica bundles prepared in a mixture of ethanol and water under a basic condition. The lengths and diameters of the bundles were tens of micrometers and 100–200 nm, respectively. Figure 7b shows that the coiling pore channels were parallel to each other and the helical pitches were around 400–500 nm.

Figure 8a shows the FESEM image of the left-handed helical mesoporous silica bundles prepared from a mixture of 10 mg of L-ValPyPF<sub>6</sub>, 0.4 mL of ethanol, 0.6 mL of 10.0 wt % NH<sub>3</sub> aq, and 20 mg of TEOS. The diameters of the bundles were around 200–300 nm. However, some huge bundles were also identified in the FESEM image (Figure 8a). The bundles exhibited a nitrogen BET surface area of 255 m<sup>2</sup>/g. The nitrogen BJH pore size distribution plot determined from the adsorption branch showed two peaks at 4.7 and 12 nm (Supporting Information, Figure S16). It is assumed that the small pores of 4.7 nm are due to the inner diameters of the pore channels and the large pores of around 12 nm are probably attributed to the interfiber spaces among the ultrafine fibers within the helical bundles. This large-pore mesoporous structure may be suitable for the immobilization and encapsulation of large molecules.<sup>22</sup>

Figure 8b and c shows the FESEM and TEM images of the multiple left-handed helical mesoporous silica nanofibers prepared from a mixture of 10 mg of L-ValPyPF<sub>6</sub>, 0.5 mL of ethanol, 0.5 mL of 10.0 wt % NH<sub>3</sub> aq, and 20 mg of TEOS. A kind of hierarchical nanostructure was identified. First, left-handed coiled or twisted ribbons were constructed by ultrafine nanofibers. Next, the ribbons changed to bundle structure by reconstruction (Figure 8b). The TEM image shows that the twisted pore channels are parallel to each other in multilayer and oriented to the axis of the nanoribbon (Figure 8c). Generally, the mesoporous ribbons tended to be formed with increasing volume ratio of ethanol to water.

The helical mesoporous silica bundles were successfully prepared in the range of 4:6 to 7:3 as the volume ratio of ethanol

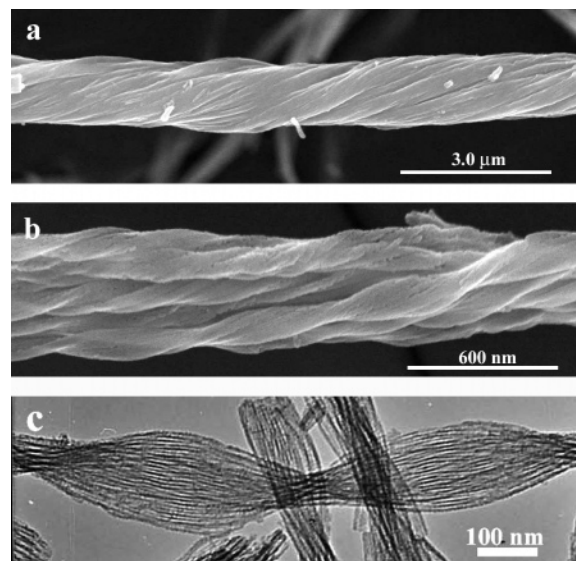


**Figure 8.** FESEM (a,b) and TEM (c) images of left-handed helical mesoporous silica bundles. Preparation condition for (a): 10 mg of L-ValPyPF<sub>6</sub>, 0.4 mL of ethanol, 0.6 mL of 10.0 wt % NH<sub>3</sub> aq, and 20 mg of TEOS. Preparation condition for (b) and (c): 10 mg of L-ValPyPF<sub>6</sub>, 0.5 mL of ethanol, 0.5 mL of 10.0 wt % NH<sub>3</sub> aq, and 20 mg of TEOS.

to water. Furthermore, the multiple helical bundles were successfully prepared in mixtures of water and other alcohols such as methanol, 2-propanol, and 1-propanol (not shown here). When the volume ratio of ethanol to water was 3:7, the obtained silica bundles showed a slight helix. On the other hand, when the sol–gel polycondensation reactions were carried out in pure water, only amorphous particles were obtained. Furthermore, when the volume ratio of ethanol to water was higher than 8:2, left-handed twisted silica nanotubes constructed by ribbons<sup>23</sup> were identified in the FESEM and TEM images (Supporting Information, Figure S17). No pore channels were identified within the ribbons (Figure S17b). The lengths of the nanotubes were around several micrometers.

The helical silica bundles were also prepared under weaker base conditions. Figure 9 shows the FESEM and TEM images of the silica bundles prepared in a mixture of ethanol and water (volume ratio: 4:6) using 5.0 and 2.5 wt % NH<sub>3</sub> aq as catalyst. The helical bundles in Figure 9a and b were prepared using 5.0 and 2.5 wt % NH<sub>3</sub> aq as catalyst, respectively. It seems that the helical structure tends to be formed under higher NH<sub>3</sub> concentrations (Figures 8a, 9a,b). The samples shown in Figure 9 show similar pore-architectures. Two kinds of pore-architectures (Figure 9c and d) were identified in these two samples. The TEM image shown in Figure 9c is similar to that shown in Figure 8c. The TEM image in Figure 9d is a kind of 2D or 3D pore-architecture, which looks like the 1D pore channels were linked through holes side by side. Unfortunately, the pore diameter of this 2D or 3D pore-architecture is too fine to be recognized more clearly in FESEM images. These two samples also showed the same nitrogen BET pore size distribution with a peak at 6.1 nm (Supporting Information, Figures S18 and S19). The bundles in Figure 9a and b exhibited nitrogen BET surface areas of 518 and 634 m<sup>2</sup>/g, respectively. Although the pore size of the samples in Figure 9 (6.1 nm) was larger than that of the sample shown in Figure 8a (4.7 nm), the surface area of the

(22) Goto, Y.; Inagaki, S. *Chem. Commun.* **2002**, 2410.

(23) Shimizu, T.; Masuda, M.; Minamikawa, H. *Chem. Rev.* **2005**, *105*, 1401.

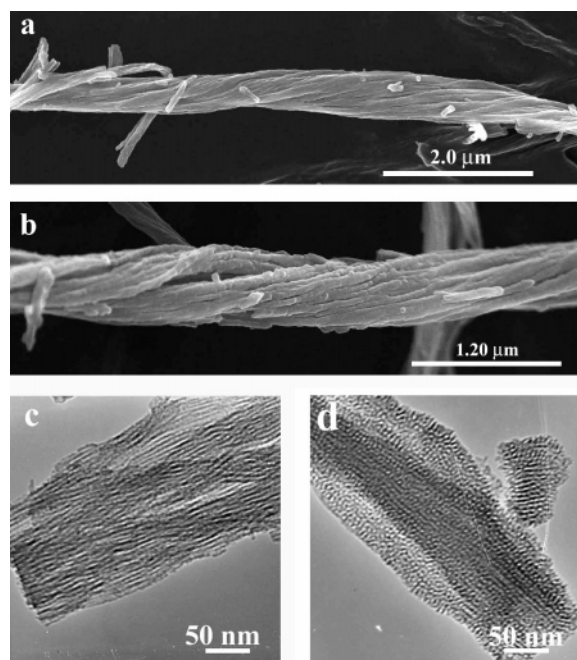


**Figure 9.** FESEM (a,b) and TEM (c,d) images of the multiple left-handed helical mesoporous silica fibers. Preparation condition for (a) and (c): 10 mg of **L-ValPyPF<sub>6</sub>**, 0.4 mL of ethanol, 0.6 mL of 5.0 wt %  $\text{NH}_3$  aq, and 20 mg of TEOS. Preparation condition for (b) and (d): 10 mg of **L-ValPyPF<sub>6</sub>**, 0.4 mL of ethanol, 0.6 mL of 2.5 wt %  $\text{NH}_3$  aq, and 20 mg of TEOS.

sample in Figure 9 was higher than that of the sample in Figure 8a (255  $\text{m}^2/\text{g}$ ). This result also indicates that the pore-architectures are different between these samples.

To clarify this 2D or 3D pore-architecture using FESEM, we synthesized **bola-L-ValPyPF<sub>6</sub>** according to the literature<sup>24</sup> and prepared silica nanotubes using the self-assemblies as template (Supporting Information, Scheme S2). The **bola-L-ValPyPF<sub>6</sub>** can form physical hydrogel in water, and the minimum gel concentration is 28  $\text{g}/\text{dm}^3$  at 25 °C. By changing the molar ratio of TEOS to **bola-L-ValPyPF<sub>6</sub>**, nanotubes with holes in the walls were successfully prepared (Figure 10). The 2D and 3D pore-architectures were obtained in which the nanotubes linked with the neighbors through the holes. The formation of silica nanotubes using template method is based on several steps such as the adsorption and polymerization of silica oligomers on the surface of templates.<sup>25</sup> If only few silica oligomers exist in the reaction mixture, it is reasonable to form holes when these oligomers polymerize on the surface of templates.

On the basis of the results of the preparation of nanotubes above, we tried to prepare the 2D or 3D pore-architectures under dilute reactants and lower weight ratio of TEOS to **L-ValPyPF<sub>6</sub>** conditions. The FESEM and TEM images of the obtained silica were shown in the Supporting Information, Figure S20. The sample in Figure S20a was prepared from a mixture of 40 mg of **L-ValPyPF<sub>6</sub>**, 1.6 mL of ethanol, 2.4 mL of 5.0 wt %  $\text{NH}_3$  aq, and 30 mg of TEOS. The loosely left-handed helical bundles were constructed into loosely coiled fine ribbons (Figure S20a). TEM images indicate that the 1D helical pore channels are linking with neighbors through the holes in the walls (Supporting

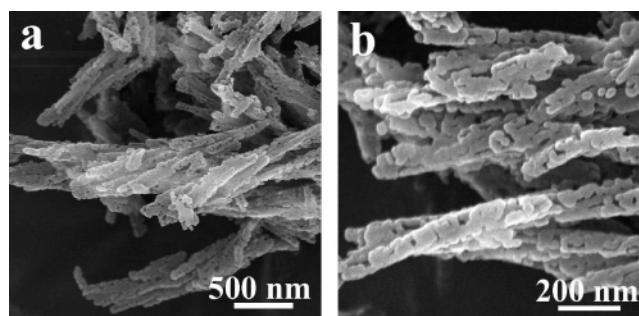


**Figure 10.** FESEM images of silica nanotubes. Preparation condition: 30 mg of **L-9Val6PyPF<sub>6</sub>**, 1.0 mL of 1.0 M HCl aq, and 50 mg of TEOS.

Information, Figure S20b and c). Although some bundles of this sample show TEM images similar to that of Figure 9c, bundles more than 70% show this 2D/3D pore-architecture. When the weight ratio of TEOS to **L-ValPyPF<sub>6</sub>** was increased to 4:6, about 10% of bundles show 2D or 3D pore-architectures (Figure S20d). The nitrogen BET surface areas of the samples shown in Figure S20a and d were 705 and 551  $\text{m}^2/\text{g}$ , respectively. Also, the pore size distribution plots of these two samples showed a peak around 6–7 nm (Supporting Information, Figures S21 and S22).

These results indicate that not only the concentration of  $\text{NH}_3$  aq but also the weight ratio of gelator to TEOS can affect the pore-architectures. There is another possibility to form the present 2D/3D pore-architecture. The holes in the walls of nanotubes may be formed during the calcination procedure. Although some gelator molecules are washed off with methanol, some of them still remain within the silica tube. During calcination, the hexafluorophosphate would decompose,<sup>26</sup> and the obtained fluoride would etch the silica walls. More research should be carried out to study these special 2D/3D chiral pore-architectures.

**Results of SAXS.** Some of these helical mesoporous silica nanostructures have been studied using small-angle X-ray scattering. Because the ribbons are in nanosize and they are constructed by nanotubes in monolayer, these nanotubes did not pack in high period. Generally, we can only recognize one broad peak at low angle (unpublished results). When the pore-diameter is too large, the peak appears at the slope of the curve line and is difficult to recognize (Supporting Information, Figures S23 and S24). In the sample shown in Figure 20d that showed 2D/3D chiral pore-architecture, two broad peaks were found at 1.5 and 1.0 nm in the SAXS graph (Supporting Information, Figure S24).

## Conclusion

Twisted mesoporous silica nanoribbons have been successfully prepared using a chiral cationic thickener **L-ValPyBr**. The nanoribbons are uniform with respect to width, thickness, and helical pitch without combining small particles. The helical pitch of the ribbons was able to be changed by varying the ratio of alcohols to water of the reaction mixtures. These twisted silica nanoribbons tended to reconstruct into bundles by stirring during the synthetic process. Left-handed helical mesoporous silica nanofibers have been prepared in mixtures of ethanol and water using the self-assemblies of a gelator **L-ValPyPF<sub>6</sub>** as template. TEM images showed that the pore channels were parallel to each other. Under the conditions of dilute reactants and lower

(24) Suzuki, M.; Owa, S.; Yumoto, M.; Kimura, M.; Shirai, H.; Hanabusa, K. *Tetrahedron Lett.* **2004**, *45*, 5399.

(25) Jung, J. H.; Amaike, M.; Shinkai, S. *Chem. Commun.* **2000**, 2343.

(26) Watanabe, M.; Asai, N.; Sakurai, M.; Maeda, M. *Phosphorus Res. Bull.* **1998**, *8*, 1.

weight ratio of TEOS to L-ValPyPF<sub>6</sub>, a 2D or 3D pore-architecture, which was formed by 1D chiral and helical pore channels linking through the holes in the walls, was prepared.

**Acknowledgment.** We thank Prof. Hiroshi Uraka, Kyoto Institute of Technology, for taking SAXS graphs. This work was supported by the Grant-in-Aid for 21st Century COE Program by the Ministry of Education, Culture, Sports, Science, and Technology of Japan.

**Supporting Information Available:** Experimental section: FESEM images of short silica nanorods and left-handed twisted nanoribbons prepared in the mixture of 2-propanol and water; FESEM image of silica flakes prepared in the mixture of ethanol and water; BET results of silica nanoribbons and bundles; FESEM image of silica nanotubes prepared in the mixture of 1-propanol and water; and SAXS results of samples. This material is available free of charge via the Internet at <http://pubs.acs.org>.

JA064240B